Transcatheter closure of inferior sinus venosus defect using a patent ductus arteriosus occluder following simulation with a 3D-printed model

Zeming Zhou[1,2#], Yuanrui Gu[3#], Hong Zheng[1], Huijun Song[1], Shiguo Li[1], Chaowu Yan[1], Zhongying Xu[1]

[1]Department of Structural Heart Disease, State Key Laboratory of Cardiovascular Disease, Fuwai Hospital, National Center for Cardiovascular Diseases, Chinese Academy of Medical Sciences, Peking Union Medical College, Beijing, China; [2]Department of Cardiology, State Key Laboratory of Cardiovascular Disease, Fuwai Hospital, National Center for Cardiovascular Disease, Chinese Academy of Medical Sciences, Peking Union Medical College, Beijing, China; [3]Department of Vascular Surgery, State Key Laboratory of Cardiovascular Disease, Fuwai Hospital, National Center for Cardiovascular Disease, Chinese Academy of Medical Sciences, Peking Union Medical College, Beijing, China

Contributions: (I) Conception and design: H Zheng, Z Zhou; (II) Administrative support: H Zheng; (III) Provision of study materials or patients: H Song, S Li, C Yan, Z Xu; (IV) Collection and assembly of data: Y Gu; (V) Data analysis and interpretation: Y Gu; (VI) Manuscript writing: All authors; (VII) Final approval of manuscript: All authors.

[#]These authors contributed equally to this work as co-first authors.

Correspondence to: Hong Zheng, MD. Department of Structural Heart Disease, Fuwai Hospital, National Center for Cardiovascular Disease, Chinese Academy of Medical Sciences and Peking Union Medical College, No. 167, Beilishi Road, Beijing 100037, China. Email: zheng_hung@126.com.

Background: Transcatheter closure of inferior sinus venosus defect (ISVD) is still contraindication. To explore whether transcatheter closure with patent ductus arteriosus (PDA) occluders is possible for ISVD.

Methods: From June 2014 to March 2021, 12 patients were recruited diagnosed as <25 mm ISVD. The three-dimensional printing (3DP) heart model was produced based on multi-slice computed tomography (MSCT) scans. Preoperative closure simulation was planned on the personalized 3D model for each patient. Follow-up including electrocardiography (ECG), transthoracic echocardiography (TTE), and X-ray was traced.

Results: 3DP models of 12 patients were successfully printed. Twelve patients had been diagnosed with <25 mm ISVD and 4 of them had another secundum atrial septal defect (ASD). All patients were produced interventional therapy successfully. PDA occluder was implanted to closed ISVD, and ASD was closed using ASD occluder simultaneously. The average diameter of ISVD measured by TTE was (12.67±3.80), and the average diameter of sagittal axes and longitudinal axes measured by the 3D-printed model was (17.08±3.20) and (18.42±4.62) mm, respectively. The average size of PDA (diameter of pulmonary artery side) was (28.17±3.35) mm. Compared with the preoperative, the X-ray cardiothoracic ratio (0.51±0.04 *vs.* 0.47±0.06, P=0.007) and the right ventricle anterior-posterior diameter (31.17±5.65 *vs.* 24.58±3.75 mm, P<0.001) of postoperative was significantly decreased. During the average (47.75±27.52) months follow-up, it has achieved satisfying results, and there were no severe adverse events such as device transposition, death, and pericardial tamponade occurred.

Conclusions: Assisting by 3D heart model, transcatheter closure of ISVD with PDA occluder had an excellent outcome. This method provides a new considerable treatment strategy for ISVD.

Keywords: Three-dimensional printing (3DP); inferior sinus venosus defect (ISVD); interventional therapy; patent ductus arteriosus occluder (PAD occluder)

Introduction

Inferior sinus venosus defect (ISVD) is a rare form of congenital heart disease which is usually detected accidentally. Unlike secundum atrial septal defect (ASD), ISVD is characterized by anomalous interatrial communication between the right pulmonary veins (RPVs) and right atrium (RA) or the inferior vena cava (IVC) and RA junction (1,2). Transcatheter closure has become the preferred strategy for addressing secundum ASD since King *et al.* (3) first attempted the procedure using a double-umbrella device, demonstrating its feasibility. Transcatheter devices and delivery techniques have undergone rapid development over the last 40 years. Since the relatively recent invention and application of the ASD occluder, occlusion has become the first-choice strategy for treating ASD, and several studies have shown that the therapeutic effects of surgery and transcatheter closure are similar (4-8).

However, transcatheter closure of ISVD has been less successful, and ASD occluders are not suitable for closing ISVDs given that they are susceptible to exfoliation and transposition. Thus, most physicians still believe that surgical repair remains the recommended strategy for ISVD, and the current guidelines list transcatheter closure as contraindicated. Nevertheless, under the guidance of three-dimensional printing (3DP) technology, Dr. Yang and colleagues discovered that the most suitable device for ISVD closure was the patent ductus arteriosus (PDA) occluder, which was first successfully implanted into the human body in September 2014 (9). Dr. He reported similar success in subsequent cases (10) with only 5 cases and the description of the structure is vague.

In the present retrospective study, we aimed to investigate the feasibility and effectiveness of the PDA occluder for ISVD intervention using 3DP models. We present the following article in accordance with the STROBE reporting checklist (available at https://jtd.amegroups.com/article/view/10.21037/jtd-21-1782/rc).

Methods

Study population

This study was conducted by the Department of Structural Heart Disease of the Fuwai Hospital and informed consent was taken from the patients or legal guardians. From January 2014 to March 2021, 12 consecutive patients were diagnosed with ISVDs <25 mm in diameter, and all were referred to our structural heart disease department for interventional treatment. (The maximum ISVD diameter was selected based on the size limitations of the occluder, which has a maximum size of only 32 mm.) All patients underwent X-ray imaging, electrocardiography (ECG), transthoracic echocardiography (TTE), and multi-slice computed tomography (MSCT). The study was conducted in accordance with the Declaration of Helsinki (as revised in 2013). The study was approved by institutional ethics board of Fuwai Hospital (No. 2021-1452).

Diagnostic criteria for ISVD

The diagnostic criteria for ISVD were as follows: (I) defect located at the posterior or inferior wall of the atria with no posterior or inferior rim; (II) defect connecting the RPV(s) to the RA, or confluent with the IVC–RA junction; and (III) presence of a well-developed septum primum covering the fossa ovale without fenestrations (2).

Inclusion and exclusion

The indications for inclusion were: (I) clinical symptoms associated with cardiac overload performance; (II) the delivery sheath could pass through the inferior vein cava; (III) age >3 years. Exclusion criteria: (I) other cardiac diseases need surgery repair; (II) resistance pulmonary hypertension; (III) the longest diameter of the defect ≥25 mm.

MSCT examination

Electrocardiographic gated contrast-enhanced MSCT (SOMATOM Definition Flash, Siemens Healthcare, Germany) was performed to assess the coronary arteries and ISVD (11-13). Patients with other cardiovascular diseases (especially anomalous pulmonary vein connection and ostium primum defect) were excluded based on MSCT images. During imaging, the ideal patient heart rate was <80 bpm; 25–50 mg metoprolol was administered 30 minutes to 1 hour before scanning if the heart rate was >80 bpm. Iopamidol was intravenously injected into the median cubital vein. All images had a slice thickness of 0.625 mm and were saved in Digital Imaging and Communications in Medicine (DICOM) format. Surrounding rims were clearly visible on images in which the inferior rims and defect diameters were accurately measured by the work station. The relationships between defects and their surrounding structures were also visualized to assess whether the devices affected mitral valve function or pulmonary vein return. The initially selected

patients were based on the reconstruction of MSCT, and the one with inclusion criteria was to proceed 3DP model.

3DP models

The 3DP model was based on end-systolic MSCT images. The procedure was as follows: first, the MSCT data were imported into Mimics Research 20.0 (Materialise NV, Leuven, Belgium). A mask was created with a threshold of 266 to 3,071 Hounsfield units, following which it was cropped to remove the rib and spine through the median sagittal, coronal, and longitudinal sections. The mask was regionally expanded, and a new mask containing only cardiac parts was created. Holes caused by asymmetric distribution of the radiocontrast agent were filled by editing the mask slice-by-slice to elevate the quality and accuracy of the 3DP model. Finally, the remaining mask was calculated for a 3D model, and the data were saved in standard tessellation language (STL) format. The STL data were then imported into 3-Matic Research 12.0 (Materialise NV, Leuven, Belgium) to undergo further processing. The surface of the virtual 3D model was smoothed using the appropriate parameters, and the model was wrapped with proper parameters and hollowed. The model was then trimmed into several parts to review the internal structure and convenience of printing. The file was imported into a desktop-fused deposition modeling 3D printer (DT-150, Ningbo Trandomed Technology Co., Ltd., Ningbo, China) using a stereolithography technique, and the model was printed in photo-reactive resin polylactic acid. The actual 1:1 model was completed after 4–7 hours of printing, depending on the accuracy of the model.

Preoperative closure simulation and devices

Different occluders were implanted in the 3D model using a delivery system via the IVC. Following implantation, the deformation of the occluder and its influence on the surrounding structures (e.g., mitral valve compression, pulmonary vein or IVC obstruction, etc.) were examined. The device was defined as appropriate if it (I) completely occluded the defect, (II) did not compress or obstruct the pulmonary vein, and (III) remained stable with sufficient size.

Finally, the ASD occluder and PDA occluder were simulated using the 3D model. The two occluders used in our institution were produced by Lifetech Scientific Co., Ltd. (Shenzhen, China) or Starway Medical Tec Co., Ltd. (Beijing, China). The PDA occluder was similar to the Amplatzer Duct Occluder I, while the ASD occluder was similar to the Amplazter Septal Occluder.

During the simulation, a PDA occluder was sent to implant in the defect via an ASD sheath. The occluder size was beginning from 6 mm larger than the defect and underwent a pull-push test to examine the stability and safety after implantation. Once the occluder passed the exam, this device was chosen to implant in the patient.

Right heart catheterization and transcatheter closure

Under local or general anesthesia (<7 years of age), all patients underwent fluoroscopy-guided procedures. The right femoral vein was punctured and inserted into the puncture sheath. Routine right heart catheterization was performed, and a 6F MPA2 catheter was inserted into the pulmonary artery and right ventricle to measure pressure. Heparin (100 IU/Kg) was injected >200 s before device implantation. ISVDs were closed using a PDA occluder, and secundum ASDs were closed using an ASD occluder (Lifetech Scientific Co., Ltd. Shenzhen, China or Starway Medical Tec Co., Ltd. (Beijing, China). An occluder 8–12 mm larger than the average of the sagittal and longitudinal axes was selected in each case. A dose of 10 U/Kg per hour of low-molecular-weight heparin was administered to all patients for 24 h, and oral aspirin was administered at a dose of 200 or 100 mg/day aspirin and 75 mg/day clopidogrel for 6 months. TTE, X-ray imaging, and MSCT were performed prior to discharge. *Figure 1* shows the procedure for transcatheter closure of ISVD using a PDA occluder.

Follow-up

All patients were followed up four times over the first 12 months (1, 3, 6, and 12 months), following which they were followed up every 1 or 2 years. Arrhythmia was monitored using ECG. TTE was performed to detect the position and stability of the occluder and residual shunting, and to measure the anterior–posterior diameter of the right ventricle. X-ray imaging was performed to calculate the cardiothoracic ratio. MSCT was repeated to check the stability of the occluder and assess morphological changes.

Statistical analysis

SPSS 26.0 Statistical software (IBM Corp, Armonk, NY, USA) was used for data analysis. Continuous variables are expressed as the mean ± standard deviation (SD),
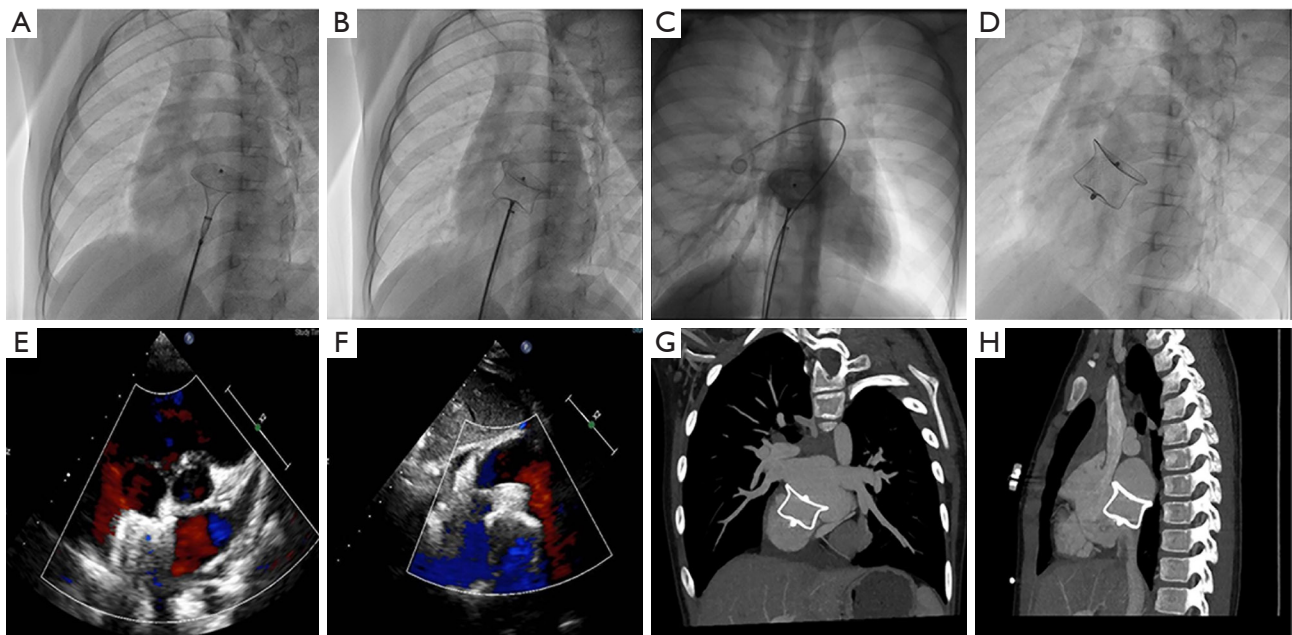
Figure 1 It has shown the procedure for transcatheter closure (A-D), post-operative TTE (E,F), and the MSCT before discharge (G,H). One of the most important indications is that the waist must be appressed to ensure success. A push–pull test should be performed under fluoroscopy to ensure stability (A,B). If necessary, pulmonary angiography should be performed to verify whether the RPV return has been affected (C). Release of the occluder (D). Post-operative TTE shows the stability of the PDA occluder and an absence of residual shunting (E,F). MSCT shows obstruction of blood recirculation (G,H). TTE, transthoracic echocardiography; MSCT, multi-slice computed tomography; RPV, right pulmonary vein; PDA, patent ductus arteriosus.

Table 1 Baseline patient characteristics

Variables	Value
Patients (n)	12
Female, n [%]	6 [50]
Age (years), mean ± SD	39.6±17.7
BMI, (kg/m^2), mean ± SD	22.46±3.48
Previous surgical repair (n)	3
Accompanying with secundum ASD (n)	4

BMI, body mass index; ASD, atrial septal defect.

while categorical variables are expressed as numbers and percentages. Clinical data such as the anterior–posterior diameter of the right ventricle and cardiothoracic ratio between the pre- and post-operative periods were assessed using paired-samples t-tests. Statistical significance was set at $P<0.05$.

Results

Patient characteristics

Ultimately, 12 patients (6 male, 6 female; average age: 39.6±17.7 years; range, 8 to 70 years). Three patients had large residual shunts several years after surgical repair. The average length of hospital stay was 3.67±1.44 days. The baseline characteristics of the patients are shown in *Table 1*.

Preoperative closure simulation

All the patients underwent the simulation, and we found the deeper the depression, the harder it is to push the device in the push and pull test. Thus, in the simulation, adding 8mm larger is safe. Even adding 12 mm was necessary for the larger defect.

Two types of devices were tested on the 3DP model, and representative simulation results for the first patient recruited in 2014 (whose ISVD diameter is shown in *Table 2*)

Table 2 Occluder size and IVSD diameter measured via TTE and 3DP modeling

Patient	Age (years)	Gender	TTE (mm)	3DP Model		Mean PAP (mmHg)	PDA occluder size (pulmonary end) (mm)	Manufacturer	Delivery sheath
				Sagittal axis (mm)	Longitudinal axis (mm)				
1	8	Male	16	15	20	16	24	Starway	14F
2	52	Male	14	18	20	19	24	Starway	14F
3	41	Male	17	17	23	11	32	Lifetech	14F
4	70	Male	11	17	10	19	24	Starway	14F
5	29	Female	11	19	24	22	32	Lifetech	14F
6	39	Male	18	15	23	22	30	Lifetech	12F
7	47	Female	12	10	18	28	30/[24][†]	Lifetech	14F
8	35	Female	9	17	16	19	32	Lifetech	14F
9	45	Female	18	24	17	17	30	Lifetech	12F
10	9	Female	10	17	21	23	28	Lifetech	12F
11	48	Male	8	18	10	14	24	Lifetech	12F
12	52	Female	8	18	19	17	28	Lifetech	14F

[†], in Patient 7, a 24/26 mm device was in planted but fell off, and implanted a 30/32 mm device successfully. IVSD, inferior sinus venosus defect; TTE, transthoracic echocardiography; 3DP, three-dimensional printing; PAP, pulmonary artery pressure; PDA, patent ductus arteriosus.
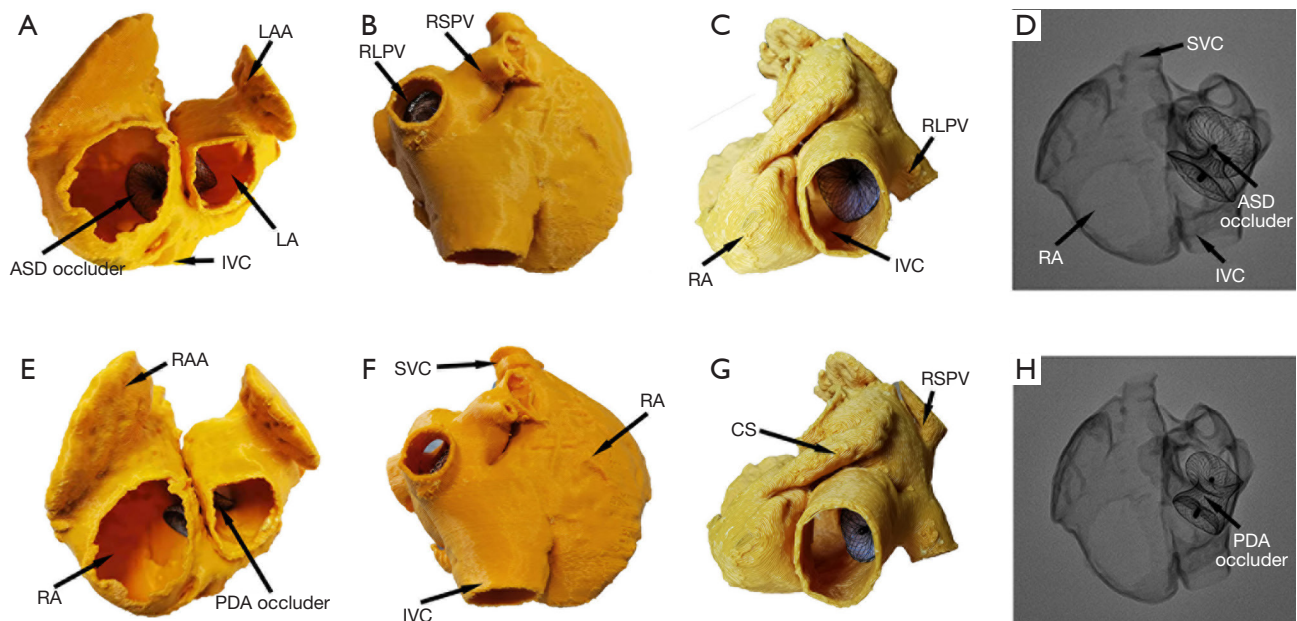

Figure 2 (A-D) The 3DP simulation for the ASD occluder, while (E-H) show that for the PDA occluder. (A,B) Show the position of the occluder from the front view. (B,F) Show complete obstruction of RPV return using the ASD occluder yet slight obstruction using the PDA occluder. (C,G) Show that obstruction of IVC return was less substantial for the PDA occluder than for the ASD occluder. (D,H) Show the position and shape of each occluder under fluoroscopy when implanted in the 3DP model. LAA, left atrial appendage; LA, left atrium; IVC, inferior vena cava; ASD, atrial septal defect; RLPV, right lower pulmonary vein; RSPV, right superior pulmonary vein; RA, right atrium; RAA, right atrial appendage; PDA, patent ductus arteriosus; SVC, superior vena cava; CS, coronary sinus.
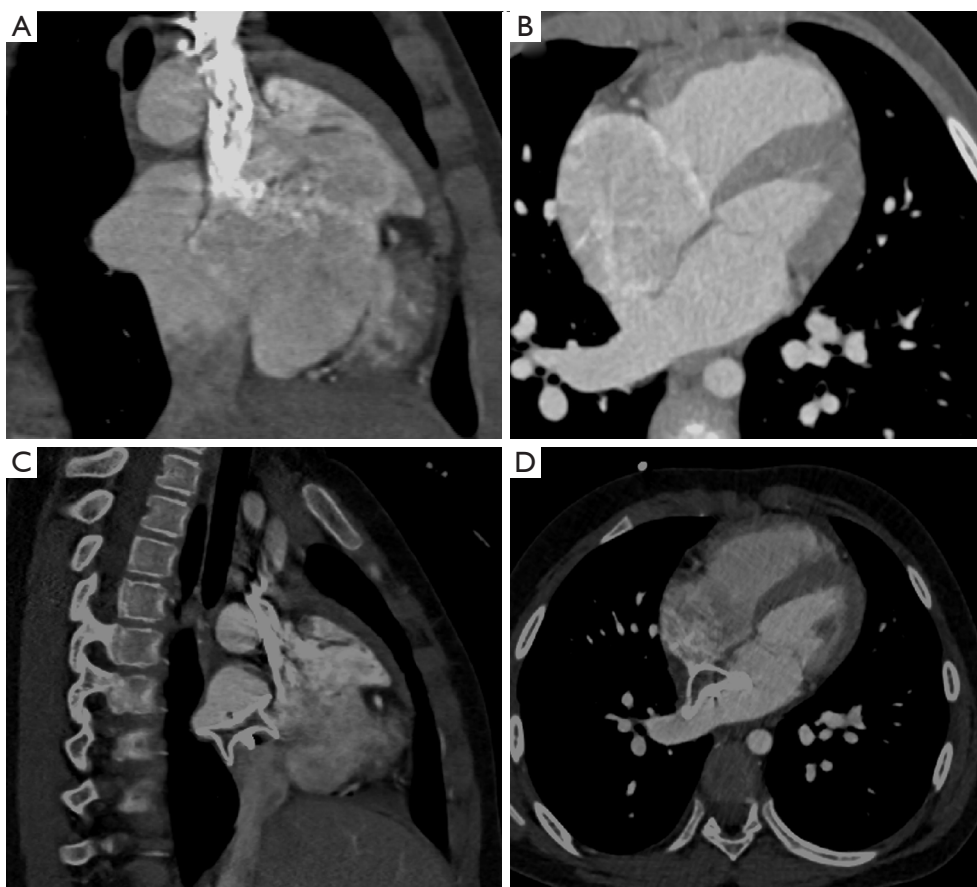
Figure 3 Preoperative (A,B) and postoperative (C,D) MSCT images. (C,D) Show no obstruction of the IVC or RPV. MSCT, multi-slice computed tomography; IVC, inferior vena cava; RPV, right pulmonary vein.

are shown in *Figure 2*. MSCT images obtained before and after surgery are shown in *Figure 3*. A 26-mm ASD occluder and a 24/26-mm PDA occluder were implanted into the 3DP model for simulated occlusion (*Figure 2*). When the 26-mm ASD occluder was implanted in the 3DP model (*Figure 2A*), the following were observed: (I) the occluder obstructed the RPV return (*Figure 2B*); (II) the right disc covered nearly 1/2 of the IVC (*Figure 2C*); (III) and there was substantial deformation of the occluder, the waist of which was suspended and could not be tightly appressed against the posterior or inferior wall of the left atrium (LA) (*Figure 2D*). The 24/26-mm PDA occluder was also used to simulate occlusion (*Figure 2E*). The results showed that the waist of the occluder appressed well to the LA, and obstruction of the pulmonary vein and IVC was also significantly decreased when compared with that observed using the ASD occluder of the same size (*Figure 2F-2H*).

Transcatheter closure

In all patients, 3D models were accurately printed, and interventional therapy was successfully administered. Secundum ASDs were detected and closed with an ASD occluder in four patients. Only one patient implanted with a 24/26-mm PDA occluder exhibited exfoliation. In this case, the device was etched out, and the patient was successfully implanted with a 30/32-mm occluder without exfoliation. The average diameter of ISVD measured by TTE was (12.67±3.80), and the average diameter of sagittal axes and longitudinal axes measured by the 3D-printed model was (17.08±3.20) and (18.42±4.62) mm, respectively. The average size of the PDA (diameter of the pulmonary artery side) was 28.17±3.35 mm. The ISVD diameters measured via TTE and for the 3DP model are shown in *Table 2*. The 3DP model of the first patient's postoperative period is shown in *Figure 4*. No RPV or IVC obstruction was
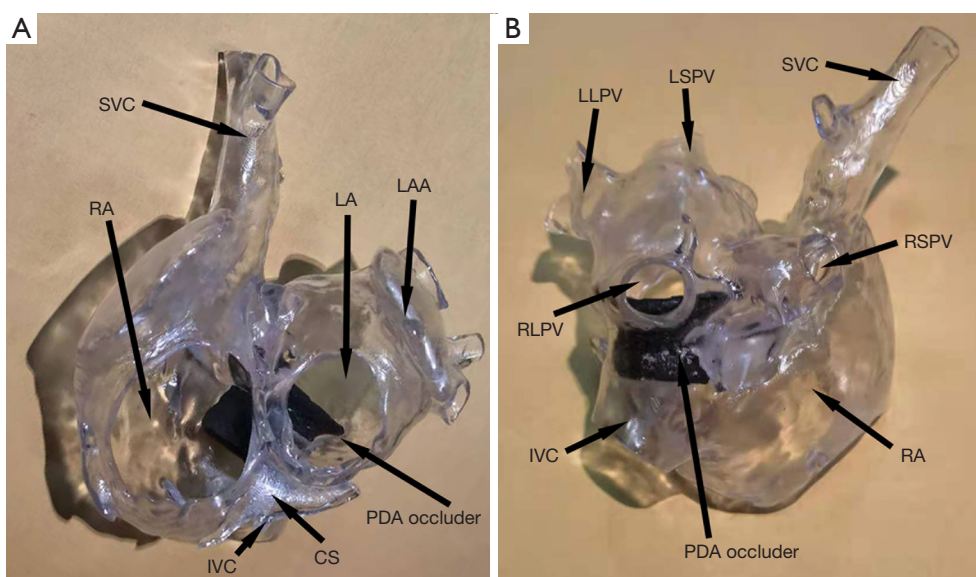
Figure 4 Position and shape of the device post-operation. No IVC (A, front view) or RPV (B, rear view) obstruction were observed following implantation of the PDA occluder. SVC, superior vena cava; RA, right atrium; LA, left atrium; LAA, left atrial appendage; IVC, inferior vena cava; CS, coronary sinus; PDA, patent ductus arteriosus; LLPV, left lower pulmonary vein; LSPV, left superior pulmonary vein; RLPV, right lower pulmonary vein; RSPV, right superior pulmonary vein.

observed following implantation of the PDA occluder.

Follow-up data

The average length of follow-up was 47.75±27.52 (range, 6–83) months. ECG findings were normal pre- and postoperatively. However, the postoperative cardiothoracic X-ray ratio was significantly lower than the preoperative value (0.51±0.04 *vs.* 0.47±0.06; P=0.007). The anterior–posterior diameter of the right ventricle on TTE 1 day after the procedure was significantly reduced when compared with that before closure (24.58±3.75 *vs.* 31.17±5.65 mm; P<0.001). All patients underwent repeated MDCT at 6 or 12 months after the procedure, which showed perfect positioning and shape of the occluders. No adverse events such as residual shunting, occluder transposition or exfoliation, or procedure-related deaths occurred during follow-up.

Discussion

Interventional therapy is a common treatment strategy for secundum ASD worldwide, and some previous studies have reported excellent outcomes following interventional and surgical closure in both adult and pediatric patients (4-8).

However, interventional treatment is associated with shorter hospital stays, lower costs, lower infection rates, and fewer complications than surgical treatment. In addition, small wounds and a short recovery period are key factors that motivate patients to prefer interventional therapy.

Previously, transcatheter closure was contraindicated in patients with ISVD. In addition to the psychological and emotional burden of surgical closure, patients with ISVD undergoing surgical closure experience worse clinical outcomes than those with secundum ASD, especially in terms of residual shunting rate, reintervention rate, and the duration of cardiopulmonary bypass and hospitalization (2). Since 2014, researchers have explored the feasibility and effectiveness of transcatheter ISVD closure, prompting reconsideration of interventional treatment in this population. The 3D models developed in the present study revealed that ISVDs are mainly present in two forms: (I) confluence of the defect with the RPV(s) and RA junction, resulting in direct pulmonary venous blood return through the defect into the RA, and an absent posterior or posterior–inferior rim in the atrial wall. These defects are often elliptical in shape, with long longitudinal axis diameters and short sagittal axis diameters. Alternatively, (II) the defect may be directly confluent with the LA and IVC, with its inferior rim consisting of the RA–IVC junction
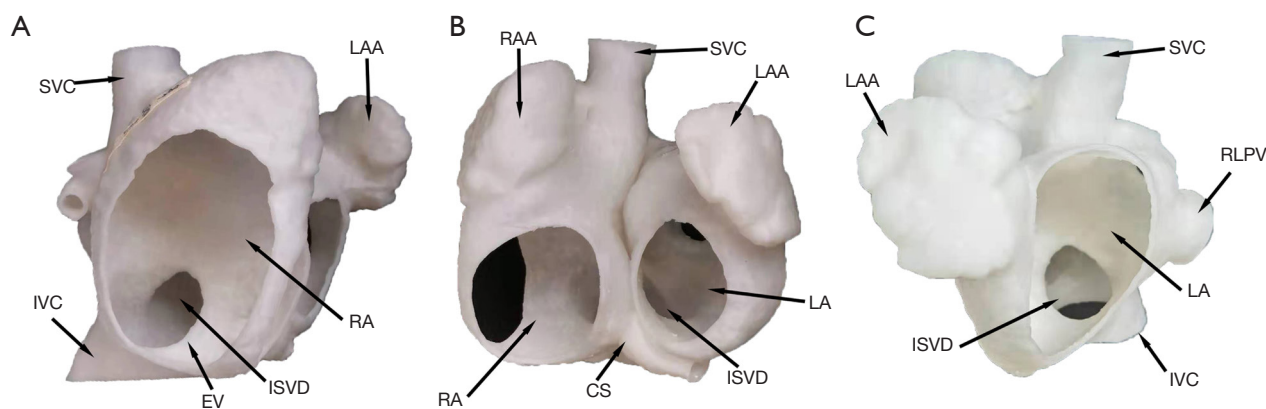
Figure 5 ISVD exhibits a semicircular shape from an RA view (A), concave disc shape from a front view (B), and a relatively regular circular shape from an LA view (C). SVC, superior vena cava; LAA, left atrial appendage; IVC, inferior vena cava; EV, eustachian valve; ISVD, inferior sinus venosus defect; RA, right atrium; RAA, right atrial appendage; CS, coronary sinus; LA, left atrium; RLPV, right lower pulmonary vein.

(similar to the "platform" anatomy) at an intersection angle >120°. The shape of the ISVD is often semicircular on RA views (*Figure 5A*), concave and disc-shaped on front views (*Figure 5B*), and relatively circular on LA views (*Figure 5C*). The posterior and inferior walls of the LA extend directly to the IVC through the ISVD. Therefore, the key to successful occlusion is to ensure that the device is stable and will not obstruct RPV return or affect the function of adjacent structures.

The present 3DP simulations indicated that the large left discs of ASDs easily obstructed RPV return, while occluder exhibited substantial deformation (i.e., suspension of the right disc and waist) (*Figure 2D*). When deployed in the atrium of the real heart, the occluder is easily transposed. Suspension of the right disc and waist may be related to the different lengths of the left and right disc skirts, which are generally 7 and 5 mm, respectively. In addition, the absence of a rim consisting of a "platform" may be insufficient for supporting the occluder.

Our morphological analysis of the 3DP models indicated that the PDA occluder is very suitable for ISVD occlusion. The PDA occluder consists of a long waist and a short, flat left disc, similar to a champagne cork. The PDA occluder seals the bottle through the friction of its ampulla. When the PDA occluder was implanted, the connection between the left disc of the occluder and the waist was squeezed by the superior and anterior rim of the defect to form a depression. At the same time, the long waist on the opposite side of the depression was tightly appressed

to the posterior atrial wall and the junction of the LA–IVC (*Figures 2H,3C,4B*). Through depression and waist friction, the increasing force provided strong support for maintaining the stability of the device. Due to the shorter skirt of the PDA occluder, it created a shallow depression at the junction of the LA–IVC and formed a platform for maintaining stability (*Figure 4B*). The waist must also be appressed, which is one of the most important indications to ensure the success of interventional treatment of ISVD via PDA occlusion (*Figures 1,3,4*). These attributes may explain why the PDA occluder is suitable for ISVD closure. When using a PDA occluder for ISVD closure, both the position of the left disc and the potential for obstruction of RPV return should be verified using intraoperative TTE. If necessary, pulmonary angiography should be performed to verify whether RPV return is affected by the recirculation of the contrast agent. Finally, in this study, a push-pull test was performed under fluoroscopy, and the occluder was released after confirming its stable position of the occluder.

In practice, in secundum ASD, the device selected was usually 4–8 mm larger than the diameter. This kind of ASD occluder keeps stable based on the tight waist and left and right disc skirt. However, the PDA occluder has only a left side disc with a short skirt. As described above, the PDA occluder keeps stable mainly through deep depression on the waist squeezed by the superior and anterior rim of the defect. The deeper the depression, the tighter appressed to the atrial wall, so the frictional force is greater. Although the definite data are lacking, we find in the simulation, the deeper the
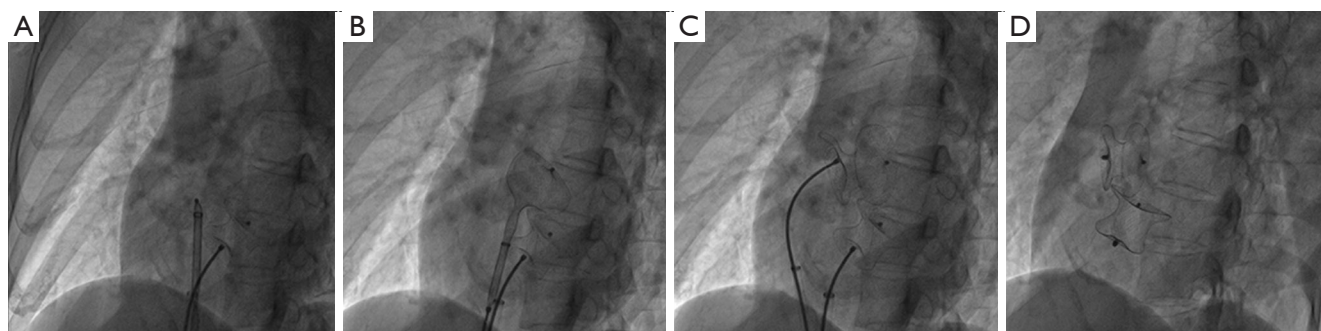
Figure 6 A patient with both ISVD and ASD. The ISVD was closed using PDA occluder (A), following which the ASD occluder was implanted to close the secundum defect. The atrial septum and left disc skirt were clamped between the left and right discs (B,C), and the two defects were closed simultaneously (D). ISVD, inferior sinus venosus defect; ASD, atrial septal defect; PDA, patent ductus arteriosus.

depression, the harder to push the device in the push and pull test. In the simulation, we begin from 6 mm larger than the defect and find that 8 mm larger is safe. Thus, according to the experience of ASD occluder 4–8 mm larger than the defect and the simulation, we find the 8–12 mm larger is safe. That is why the defect in this study was all <25 mm. The maximum size of the occluder is 34/32 mm which limited the maximum diameter of the defect that can be closed is 24 mm. this may explain why the exclusion criteria were set ≥25 mm. It was mainly limited by the current maximum device size (34/32 mm) and our previous experience. In fact, an appropriate PDA occluder size was mainly dependent on whether a clear depression formed in the waist of the PDA occluder during the operation. This suggestion is only for followers to have a reference that improves a higher success rate. Currently, we are designing larger occluders to completely solve ISVD in the future.

Although the waist of the PDA occluder is larger than that of the ASD occluder, our models indicated that the PDA occluder occupied less space (*Figures 2,3*). Furthermore, even at the same waist diameter, the PDA occluder had a single disc structure, and the maximum diameter of the left disc was smaller than the ASD occluder by approximately 10 mm. Thus, it occupied a smaller space than the ASD occluder and had a lower risk of obstructing RPV return. Additionally, the right side of the PDA had little effect on the IVC return when compared with the ASD occluder (*Figures 2H,3C,4A*). The expansion of the RA and IVC also provided sufficient space for the occluder. MSCT examination of the postoperative 3DP model for the first patient demonstrated that the PDA occluder occupied less space than we had anticipated, and there was no

obstruction of IVC return (*Figure 3C,4A*). The flat disc on the left side also did not obstruct the RPVs (*Figure 3D,4B*).

Since the study started in 2014, no serious adverse events have occurred following transcatheter closure. The most concern is the thrombotic anticoagulation and endothelialization of the occluder. During the follow-up period, oral anticoagulants were administered for 6 months. MSCT reexamination at 6 or 12 months revealed that the occluder maintained a good shape, and no signs of thromboembolism (including pulmonary embolism, etc.) were observed. In patients follow-up for more than one year, the volume and size of the right ventricle were significantly reduced, and the X-ray cardiothoracic ratio indicated that the heart function had gradually returned to normal. The erosion risk also should be concerned, especially since the left disk is probably in contact with the atrial wall. From the shape after being implanted, the occluder has slightly deformed to better fit the atrial wall. the erosion has not occurred during the follow-up period. It was considered it may be related to the flat left disc was easy to process the endothelialization. To assess long-term results, patient recruitment and follow-up are ongoing.

Four patients with IVSDs also had secundum ASDs, which were simultaneously treated with ASD occluders. For these patients, the procedure was modified as follows: (I) the PDA occluder was implanted first to close the ISVD. (II) The occluder was then pulled to fix the left disc on the atrial septum, following which (III) the ASD occluder was implanted. (IV) The atrial septal and left disc skirts were then clamped between the left and right discs (*Figure 6*). The two occluders appeared to be staggered under fluoroscopy, which improved the stability of the PDA occluder and

reduced the risk of thrombus formation. The risks of thrombosis and tissue tension were also reduced due to the decreased impact on the LA.

As shown in *Table 2*, the defect diameter measured by TTE was significantly smaller than that measured by the 3DP model, which is likely related to the operation and the patient's condition. As they were based on objective MSCT images, 3DP models could accurately measure the defect diameters. In particular, ISVDs often present as concave discs. Thus, it is necessary to comprehensively consider the diameter of the entire defect when selecting the size of the occluder, rather than based on the diameter measured by TTE alone. In this study, Patient 7 was first implanted with a 24/26-mm occluder, which fell off after the operation. The device was removed through a gooseneck snare and later replaced with a larger occluder, resulting in successful occlusion.

Importantly, 3DP has built a bridge between the real structure of the heart and the cardiologist (14,15). In this study, it had revealed that 3DP has a higher degree of accuracy than TTE, as the 3D software used can identify the shape, quantity, and position of defects automatically. However, the quality of the original MSCT data directly determines the accuracy of the model. Thus, the distribution of iopamidol and the integrity of the DICOM files are essential. It is true that the diameter can be measured on the computer, but the 3D-printed model can be directly observed and can better understand the structure. There are not many samples included in the current study, which is still a process of accumulation of experience. The defect of each patient performs in different shapes. Being responsible for each patient, we printed and performed a preoperative simulation to make a perfect plan for each patient. At the same time, the selection of patients is based on the reconstruction results on the computer. The patients with inclusion criteria process the 3D print. Therefore, the patients undergoing 3D printing are strictly selected and have the feasibility of interventional treatment. This study highlights the obvious advantages of using a 3D model to simulate PDA occlusion prior to surgery. Further cases of ISVD closure with PDA occluders are required to verify its efficacy. In addition, development of a larger PDA occluder may enable more patients with ISVD to undergo non-surgical treatment.

This study had some limitations, including its retrospective design. In addition, it was performed in a single center and enrolled only 12 patients. Long-term follow-up is still being conducted.

Conclusions

The application of 3DP in structural heart disease has progressed in recent years (16,17), and improvements in interventional devices can enable many patients with congenital heart diseases to undergo interventional therapy. Using 3DP models, the current study demonstrated that interventional therapy using a PDA occluder is feasible and effective in patients with ISVDs. Nonetheless, individualized planning and careful preoperative preparation are required. Further studies are also necessary to verify our findings and determine whether larger PDA occluders can expand indications for interventional therapy in patients with ISVDs.

Acknowledgments

Footnote

Reporting Checklist: The authors have completed the STROBE reporting checklist. Available at https://jtd.amegroups.com/article/view/10.21037/jtd-21-1782/rc

Data Sharing Statement: Available at https://jtd.amegroups.com/article/view/10.21037/jtd-21-1782/dss

Conflicts of Interest: All authors have completed the ICMJE uniform disclosure form (available at https://jtd.amegroups.com/article/view/10.21037/jtd-21-1782/coif). The authors have no conflicts of interest to declare.

Ethical Statement: The authors are accountable for all aspects of the work in ensuring that questions related to the accuracy or integrity of any part of the work are appropriately investigated and resolved. The study was conducted in accordance with the Declaration of Helsinki (as revised in 2013). The study was approved by institutional ethics board of Fuwai Hospital (No. 2021-1452) and informed consent was taken from the patients or legal guardians.

Open Access Statement: This is an Open Access article

distributed in accordance with the Creative Commons Attribution-NonCommercial-NoDerivs 4.0 International License (CC BY-NC-ND 4.0), which permits the non-commercial replication and distribution of the article with the strict proviso that no changes or edits are made and the original work is properly cited (including links to both the formal publication through the relevant DOI and the license). See: https://creativecommons.org/licenses/by-nc-nd/4.0/.

References

1. Crystal MA, Al Najashi K, Williams WG, et al. Inferior sinus venosus defect: echocardiographic diagnosis and surgical approach. J Thorac Cardiovasc Surg 2009;137:1349-55.
2. Banka P, Bacha E, Powell AJ, et al. Outcomes of inferior sinus venosus defect repair. J Thorac Cardiovasc Surg 2011;142:517-22.
3. King TD, Mills NL. Nonoperative closure of atrial septal defects. Surgery 1974;75:383-8.
4. Ooi YK, Kelleman M, Ehrlich A, et al. Transcatheter Versus Surgical Closure of Atrial Septal Defects in Children: A Value Comparison. JACC Cardiovasc Interv 2016;9:79-86.
5. Kotowycz MA, Therrien J, Ionescu-Ittu R, et al. Long-term outcomes after surgical versus transcatheter closure of atrial septal defects in adults. JACC Cardiovasc Interv 2013;6:497-503.
6. Du ZD, Hijazi ZM, Kleinman CS, et al. Comparison between transcatheter and surgical closure of secundum atrial septal defect in children and adults: results of a multicenter nonrandomized trial. J Am Coll Cardiol 2002;39:1836-44.
7. Hughes ML, Maskell G, Goh TH, et al. Prospective comparison of costs and short term health outcomes of surgical versus device closure of atrial septal defect in children. Heart 2002;88:67-70.
8. Mylonas KS, Ziogas IA, Evangeliou A, et al. Minimally Invasive Surgery vs Device Closure for Atrial Septal Defects: A Systematic Review and Meta-analysis. Pediatr Cardiol 2020;41:853-61.
9. Yang F, Zheng H, Lyu J, et al. A case of transcatheter closure of inferior vena cava type atrial septal defect with patent ductus arteriosus occlusion device guided by 3D printing technology. Zhonghua Xin Xue Guan Bing Za Zhi 2015;43:631-3.
10. He L, Cheng GS, Du YJ, et al. Feasibility of Device Closure for Multiple Atrial Septal Defects With an Inferior Sinus Venosus Defect: Procedural Planning Using Three-Dimensional Printed Models. Heart Lung Circ 2020;29:914-20.
11. Ko SF, Liang CD, Yip HK, et al. Amplatzer septal occluder closure of atrial septal defect: evaluation of transthoracic echocardiography, cardiac CT, and transesophageal echocardiography. AJR Am J Roentgenol 2009;193:1522-9.
12. Quaife RA, Chen MY, Kim M, et al. Pre-procedural planning for percutaneous atrial septal defect closure: transesophageal echocardiography compared with cardiac computed tomographic angiography. J Cardiovasc Comput Tomogr 2010;4:330-8.
13. Fraisse A, Latchman M, Sharma SR, et al. Atrial septal defect closure: indications and contra-indications. J Thorac Dis 2018;10:S2874-81.
14. Anwar S, Singh GK, Miller J, et al. 3D Printing is a Transformative Technology in Congenital Heart Disease. JACC Basic Transl Sci 2018;3:294-312.
15. Yoo SJ, Spray T, Austin EH 3rd, et al. Hands-on surgical training of congenital heart surgery using 3-dimensional print models. J Thorac Cardiovasc Surg 2017;153:1530-40.
16. Little SH, Vukicevic M, Avenatti E, et al. 3D Printed Modeling for Patient-Specific Mitral Valve Intervention: Repair With a Clip and a Plug. JACC Cardiovasc Interv 2016;9:973-5.
17. Bhatla P, Mosca RS, Tretter JT. Altering management decisions with gained anatomical insight from a 3D printed model of a complex ventricular septal defect. Cardiol Young 2017;27:377-80.